Autonomous Low Earth Orbit Satellite and Orbital Debris Tracking using Mid Aperture COTS Optical Trackers

Author - Daniel M. Azari
Electro-Optical Engineer
RC Optical Systems, Inc.

Co Author - Brad Ehrhorn
Vice President
RC Optical Systems, Inc.

Abstract Summary

Title: Autonomous Low Earth Orbit Satellite and Orbital Debris Tracking using Mid Aperture COTS Optical Trackers.
Synopsis: Low Earth Orbit (LEO) and Orbital Debris tracking have become considerably important with regard to Space Situational Awareness (SSA). This paper discusses the capabilities of autonomous LEO and Orbital Debris Tracking Systems using commercially available (mid aperture 20-24 inch) telescopes, tracking gimbals, and CCD imagers.

RC Optical Systems has been developing autonomous satellite trackers that allow for unattended acquisition, imaging, and orbital determination of LEOs using low cost COTS equipment. The test setup from which we are gathering data consists of an RC Optical Systems Professional Series Elevation over Azimuth Gimbal with field de-rotation, RC Optical Systems 20 inch Ritchey-Chrétien Telescope coupled to an e2v CCD42-40 CCD array, and 78mm f/4 tracking lens coupled to a KAF-0402ME CCD array.

Central to success of LEO acquisition and open loop tracking is accurate modeling of Gimbal and telescope misalignments and flexures. Using pro-TPoint and a simple automated mapping routine we have modeled our primary telescope to achieve pointing and tracking accuracies within a population standard deviation of 1.3 arc-sec (which is 1.1 arc-sec RMS). Once modeled, a mobile system can easily and quickly be calibrated to the sky using a simple 6-10 star map to solve for axis tilt and collimation coefficients.

Acquisition of LEO satellites is accomplished through the use of a wide field imager. Using a 78mm f/4 lens and 765 x 510 x 9mu CCD array yields a 1.28 x 0.85 degree field of view in our test setup. Accurate boresite within the acquisition array is maintained throughout the full range of motion through differential tpoint modeling of the main and acquisition imagers. Satellite identification is accomplished by detecting a stationary centroid as a point source and differentiating from the background of streaked stars in a single frame. We found 97% detection rate of LEO with radar cross sections (RCS) of > 0.5 meter*meter within the acquisition array; the vast majority falling within 0.2 degrees of center. Tests of open loop tracking revealed a vast majority of satellites remain within the main detector area of 0.38 x 0.38 degrees after initial centering

Once acquired, the satellite is centered within the main imager via offset altitude-azimuth guiding. Thereafter, real time satellite position is sequentially determined and recorded using the main imaging array. Real time determination of the SGP4 Keplerian elements are solved using non-linear least squares regression. The tracking propagator is periodically updated to reflect the solved Keplerian elements in order to maintain the satellite position near image center as needed.

These processes are accomplished without the need for user intervention. Unattended fully autonomous LEO satellite tracking and orbital determination simply requires scheduling of appropriate targets and scripted command of the tracking system.

Introduction

The evolution in computing power, position and electro-optical sensors, and the availability of high quality low cost commercial off the shelf (COTS) telescope and tracking mounts have made possible the deployment of inexpensive and rapidly deployable telescope systems to provide space surveillance information. Such systems are currently in use in the High Accuracy Network Determination Systems (HANDS)[1] to supply high accuracy angular observations of deep-space geosynchronous satellites as a supplement to the Air Force Satellite Control Network (AFSCN) ranging observations. Similarly, there is a great need to supplement the orbital data of known objects and to supplement the detection of unmapped orbital debris in low earth orbit (LEO). In this paper we describe the development and evaluation of a

completely autonomous LEO satellite and orbital debris tracker using inexpensive COTS equipment. In addition, we provide a cursory evaluation of open-loop angular observation data in real-time orbital determination.

Equipment

For this exercise, we used an RC Optical Systems 20" f/8 Ritchey-Chrétien telescope as the primary imager and a Borg 78mm f/4 ED Refractor as the acquisition telescope. Both telescopes were mounted onto an RC Optical Systems Elevation over Azimuth (EL/AZ) Tracking Mount. An Apogee U42 was used as the primary imaging camera and a Santa Barbara Instruments Group ST-402 was used for acquisition; all being low cost COTS equipment.

Site location

For the purposes of this feasibility study, development and testing was performed at the author's residence observatory located in South Florida (25.6826N, 80.2807W). This site offered the decided advantage of convenience and efficiency during these developmental stages. However, this site has characteristics that make it unsuitable for an operational satellite tracker. Most importantly, the surrounding South Florida light pollution has a profoundly negative effect on the limiting detectable magnitude, and, thus; this study is limited to brighter objects; generally, those with radar cross sections of 0.5 m^2 or greater. In addition, the roll-off style roof observatory effectively obstructed objects below approximately 30 degrees of elevation. Lastly, the unpredictable and inclement summer weather made periods of clear sky quite valuable. All aspects weighed, however, this site proved quite suitable to the mission at hand and provided invaluable results.

Control hardware and architecture

Figure 1 shows a schematic of the controller configuration. The control hardware and architecture is based around a modern sophisticated multi-axis servo motion controller. Such controllers offer many advanced features which have applicability to the mission at hand. Our design goal was to minimize and compensate any mechanical imperfections in the gimbal mount, telescope, and drive train. We thus used a dual-loop feedback servo drive systems, utilizing a pseudo-absolute 28+ bit encoder on each axis to act as feedback in the position PID servo loop, and utilizing a traditional high resolution quadrature encoder on the motor to act as feedback in the velocity PID servo loop. System resonances and bandwidth were carefully measured under full load using both position and velocity FRF analysis, and filters were introduced appropriately to optimize bandwidth.

The time source was derived from a GPS/IRIG PCI card with specified resolution and accuracy of 1 μ-sec. Time synchronization between the supervisory computer and the servo controller is maintained to within the time resolution of the servo controller's clock. The main imaging camera shutter open pulse is used to trigger an event on both computer and the servo controller, providing for accurate logs of exposure times and positions.

Atmospheric parameters are measured in real time via a connected weather station. Refraction correction is based on routines published in SLALIB 2.5-3, SLA_REFRO[2]. Refraction corrections are continually calculated based on the measured atmospheric pressure, temperature, humidity and the estimated tropospheric lapse rate.

Pointing and tracking are fully model corrected using dominant terms derived from pro-TPoint by Tpoint Software[3]. Calculated satellite look angles are fully model corrected in order to reduce tracking position errors.

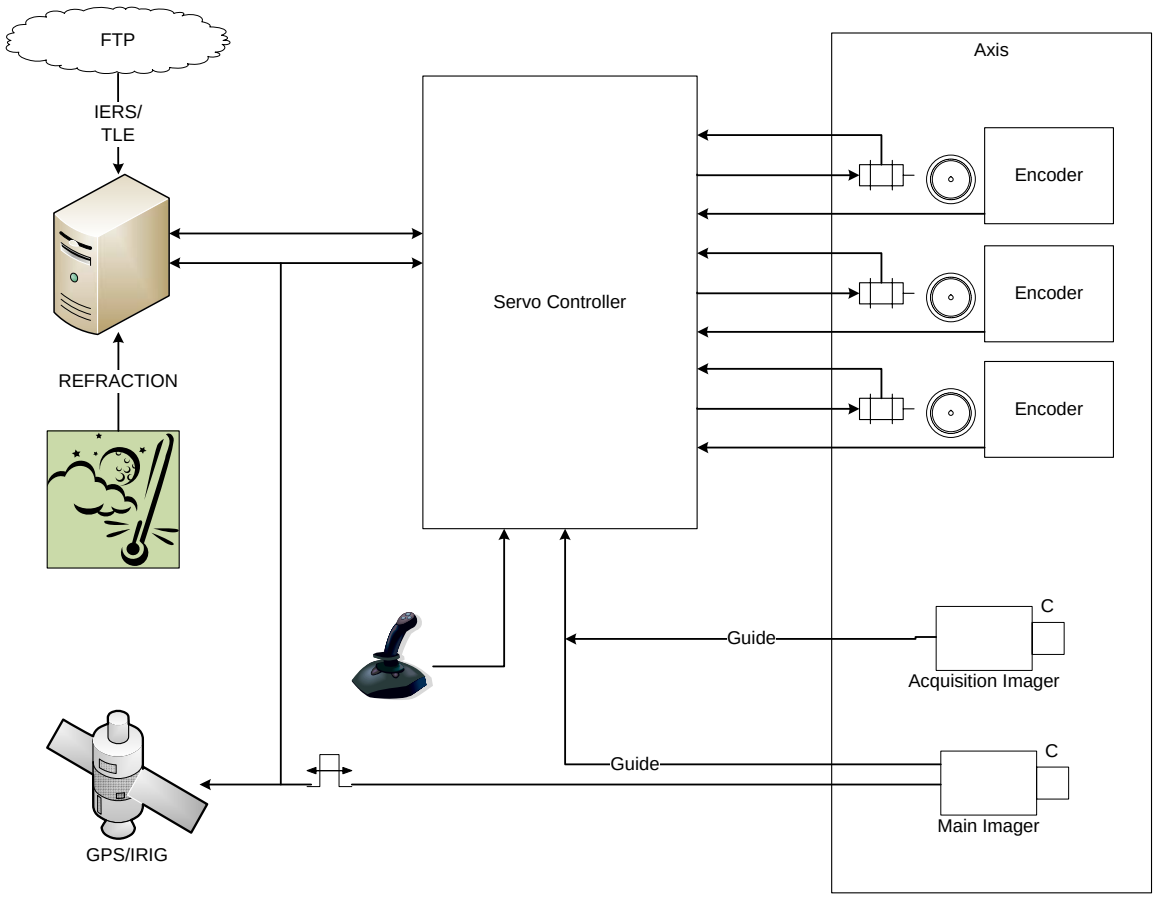

Figure 1 – Controller architecture.

Software and Propagator

All software for the control algorithms was written in Microsoft Visual C# 2005 and ACSPL+. The NORAD SGP4 propagator code is based on a C# port by Michael F. Henry[4] of the original NORAD FORTRAN SGP4 algorithms published in "Space Track Report No. 3"[5]. The SGP4 library was modified and supplemented to meet the requirements of this study.

Recent two-line elements sets (TLE) are retrieved from Space Track using the software utility "Space Track TLE Retriever" written by Dr. TS Kelso.[6]

Equipment characterization

The initial step in determining the feasibility of using completely off the shelf (COTS) equipment in an autonomous ground based electro-optical space surveillance mission was to characterize the innate pointing and tracking accuracy of the system, and to asses overall stability. Figure 2 shows the result of an approximately 90 point pro-Tpoint mapping run. Using the 'common' terms, plus a few additional harmonic terms, pro-Tpoint modeled the system to an RMS error of 1.03 arc-seconds and a population standard deviation (PSD) of 1.3 arc-seconds.

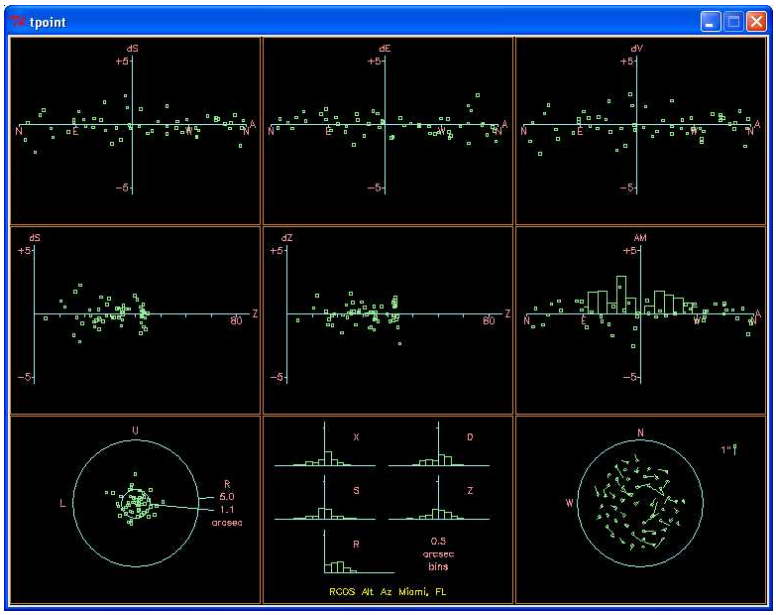

Figure 2 -- Pro-Tpoint plots of model performed on test setup, Results are RMS error of 1.03 arc-sec and population standard deviation of 1.3 arc-sec

Dynamic performance was then assessed and optimized. Since the servo configuration uses axis position encoders, drive (worm) periodic error and backlash are eliminated. The dominant dynamic error will arise from feedback resonance within the mount itself. We measured these resonances to be approximately 15-16 Hz during FRF analysis, and were effectively minimized through the prudent use notch and lag filtering techniques. Figure 3 plots the RMS position error as a fraction of tracking rate for both axes. These errors were measured on a logarithmic scale from sidereal (15 arc-sec/sec) through approximately 1 degree/sec. As expected, the fractional RMS error reduces at higher tracking rates. Again, these results are compatible with the mission at hand.

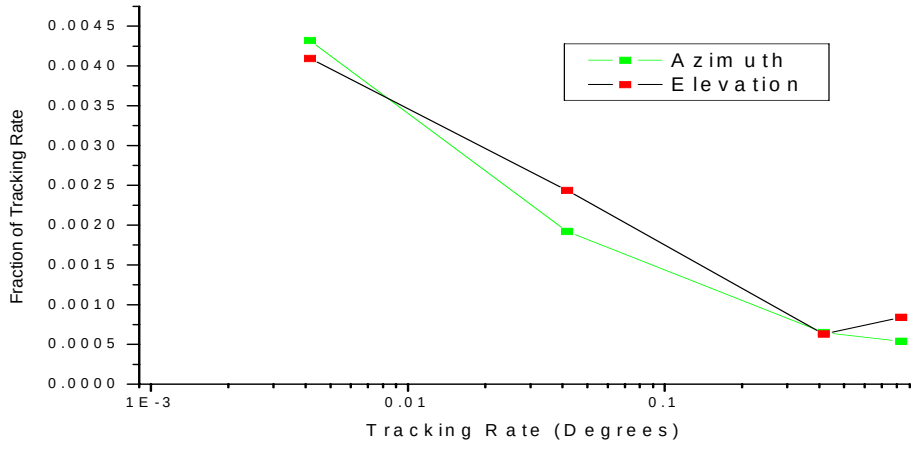

Figure 3 -- RMS position errors for Azimuth and Elevation axis expressed as a fraction of the tracking rate.

Probability of acquisition

During this stage of development we investigated the probability of detecting the targeted satellite on a wide-field acquisition camera. After much trial and error we concluded that a field of view of 1-1.5

degrees would provide a high probability of detection, while simultaneously providing the needed resolution. The equipment used for acquisition is a Borg 78mm f/4 refractor, with KAF-0402 CCD array. This combination provided a FOV of 1.3 x 0.85 degrees and a pixel resolution of 5.5 arc-seconds, and provided sufficiently fast download times.

Figure 4 shows the results of 150 LEO acquisitions. The vast majority of satellite fell near the center of the array. Approximately 3.5% of satellites where not detected, either due to insufficient brightness, or to a inaccurate orbital elements. As is seen in the histogram plot, a vast majority of satellites where detected within a radius of 0.2 degrees from center. Thus, we conclude that the chosen acquisition telescope and image array are appropriate for the mission at hand.

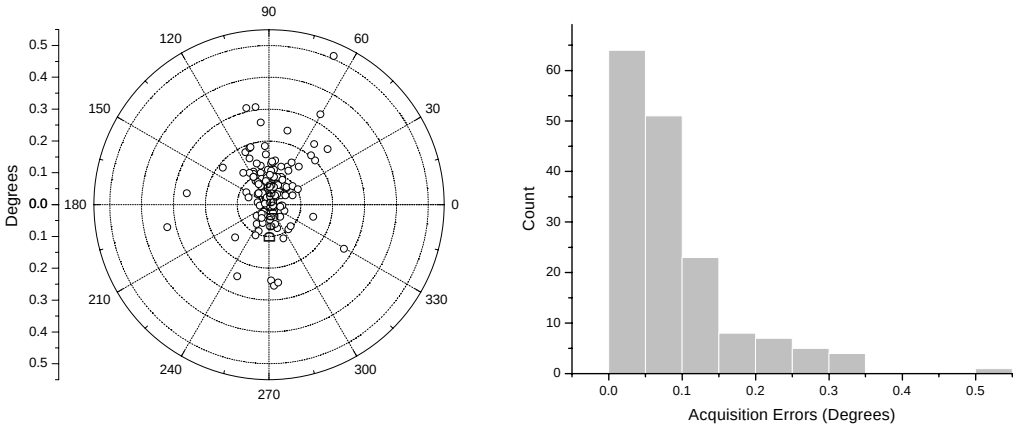

Figure 4 – Scatter plot and histogram of 150 LEO satellites acquisition positions offsets (degrees).

Open loop tracking

Open loop satellite tracking performance was subjectively measured on satellites of various altitudes and inclinations. Satellites were initially acquired at ascent through approximately 30 degrees elevation, and then were manually centered in the main imager array by either adding an offset to the TLE epoch and inclination, or by guiding in azimuth and elevation. Thereafter, the satellite position within the main imaging array was observed throughout the remainder of the transit. We observed that the vast majority of satellites remained within the main imager's FOV of 0.39 x 0.39 degrees. We therefore concluded that open loop tracking with occasional guiding corrections would be sufficient to maintain detection during automated tracking.

Automatic satellite recognition

Reliable software recognition and detection of LEO satellites against a background of streaked stars is pivotal to successful automation of LEO tracking. In a scenario of active satellite tracking, LEO are represented as image point sources. Our detection algorithm first employs image processing techniques to increase the signal to noise ratio (S/N) of the raw acquisition image. Line detection routines are then applied and detected lines are masked from the image. Satellites are then detected as the brightest point source that does not lie on a line. Detection is considered successful when the satellite position occurs within a predefined window on at least two out of four successive images. Figure 5 shows samples of the various stages of the processing procedure. Figure 5(a) depicts the raw image with a poor S/N. On this raw image, the brightest point source is detected on a star streak. Figure 5(b) shows the image processed to

improve the S/N. However, the detected point source still remains the star streak. Figure 5(c) shows the detected lines with endpoints highlighted. The satellite is now correctly identified.

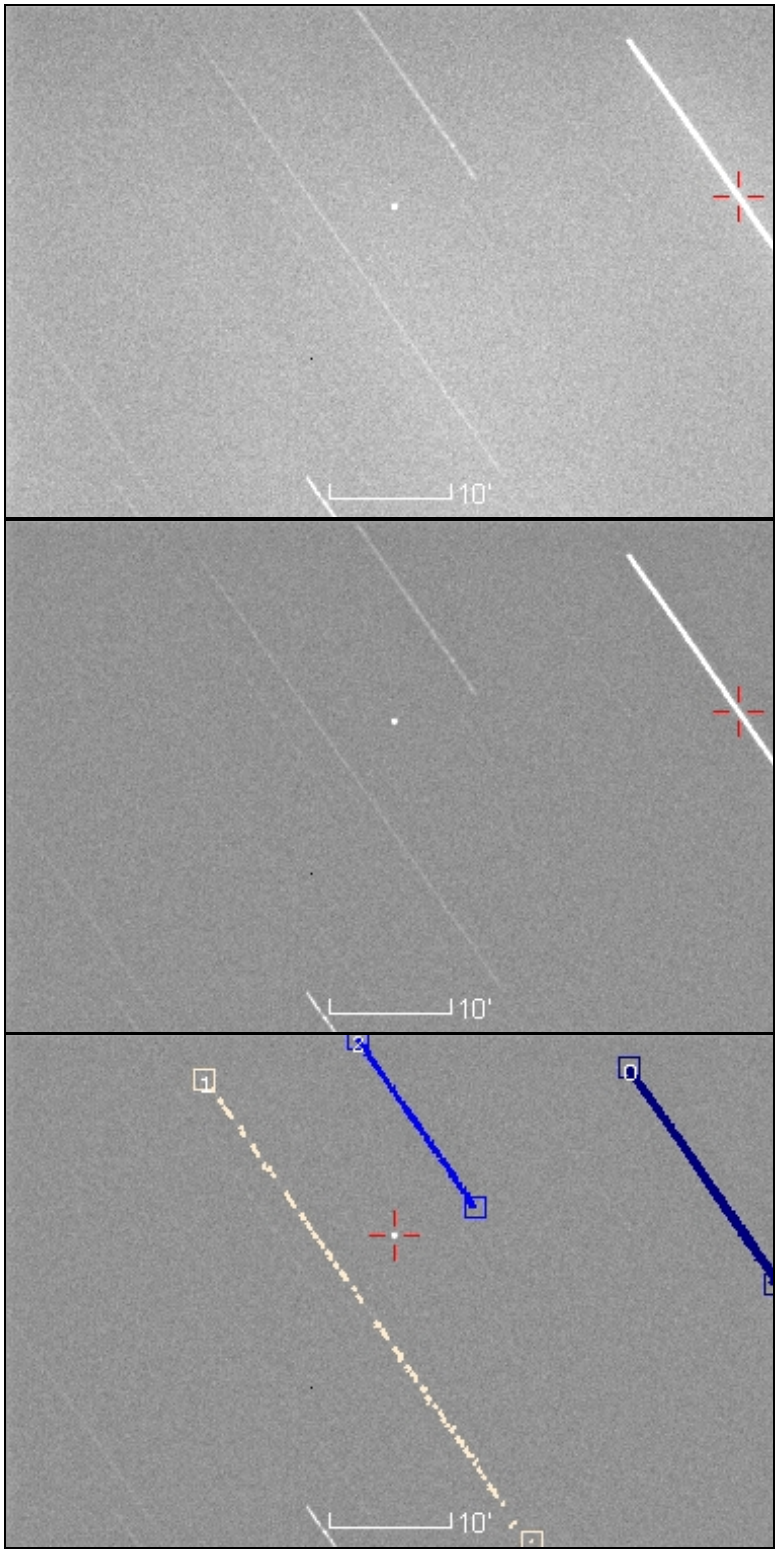

Figure 5 -- Acquisition images illustrating various stages of satellite recognition. (Top) Raw image showing poor signal to noise ratio and detected brightest object lying on star streak. (Middle) Image processed to improve signal to noise ratio. (Bottom) Line recognition and masking applied. Satellite is now properly recognized.

Autonomous control algorithm

Figure 6 shows the flow diagram of the automation algorithm. The entire process is controlled via a top level supervisory scheduler whose responsibility is to initiate an acquisition and track sequence when the next queued satellite rises above the horizon. The list of queued satellites is user defined prior to initiation of a nightly session and can be created based on several filter criteria. This is the only stage that requires user interaction.

A tracking sequence commences with a slew to the target satellite. Look angles are generated using the NORAD SGP4 propagator from the supplied two-line element. Open loop tracking is initiated and the automated satellite recognition routine loops until the recognition criteria are met. The gimbal is then commanded to offset guide to place the satellite in the center of the main imaging array, and imaging is handed over to the main imaging subsystem. In order to minimize download times and to maximize the number of collected satellite positions, the main imager is sub-framed centered on the most recent satellite position.

Satellite position on the main imaging array is detected using standard box aperture scanning for point sources. If the detected position is within the expected position error window, the image is saved and the appropriate positions and times are logged; otherwise, control is passed back to the acquisition loop. Camera shutter open and close times are accurately determined and recorded using hardware triggers on the GPS/IRIG time source. Figure 7 depicts a typical frame with saved data.

Real time orbital determination is periodically calculated on the logged position time series using simple non-linear least square fit of the SGP4 Keplerian elements to minimize look angle position and phase angles errors. Satellite bore site offsets are monitored and the tracking is compensated as required to maintain the satellite within the central 75 percent of the image array. Likewise, if the solved trajectory produces significantly reduced position errors, the solved elements can be used for active look angle generation and tracking.

Once the satellite elevation position crosses below a pre-defined limit, tracking is terminated and control is passed back to the supervisory scheduler. The sequence is repeated on the next queued satellite.

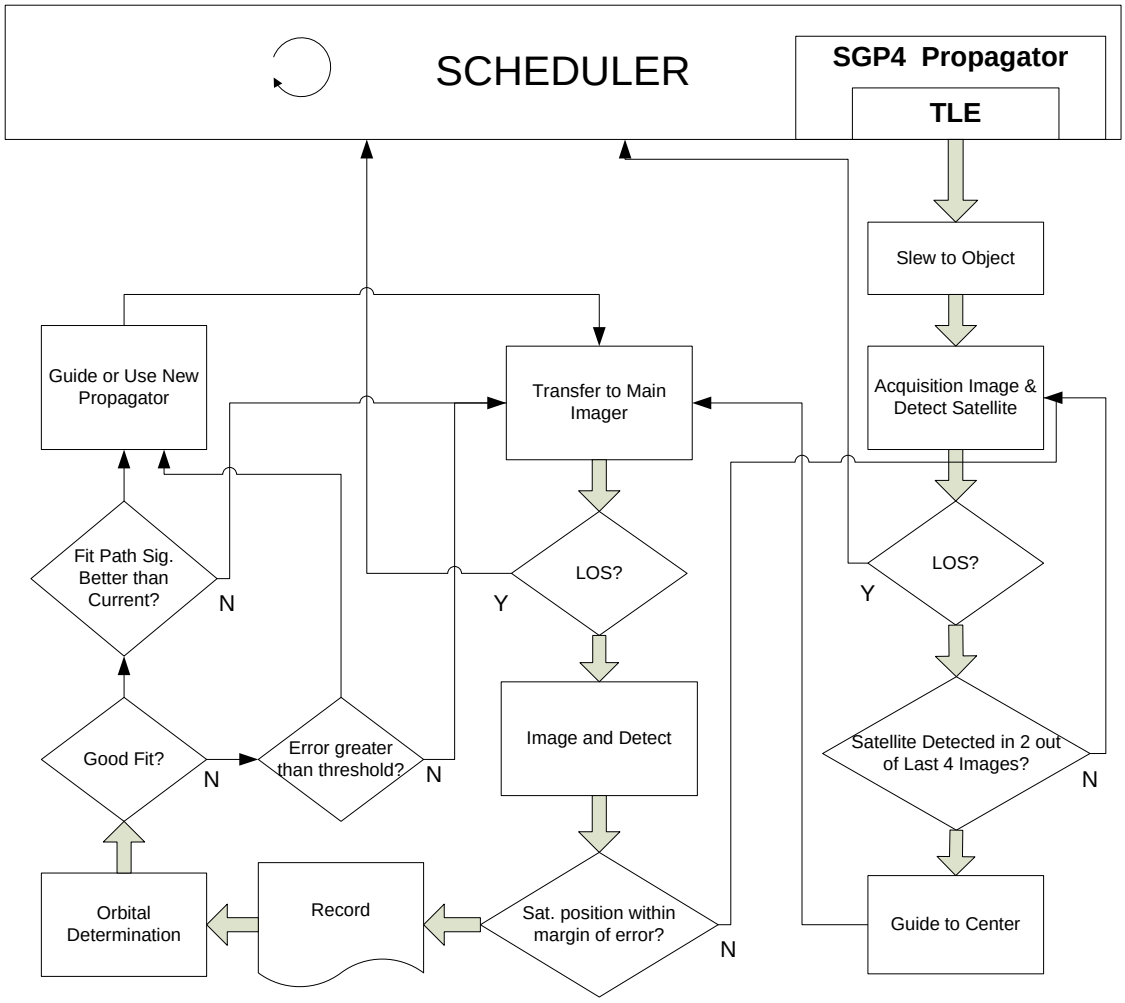

Figure 6 – Automation flow diagram

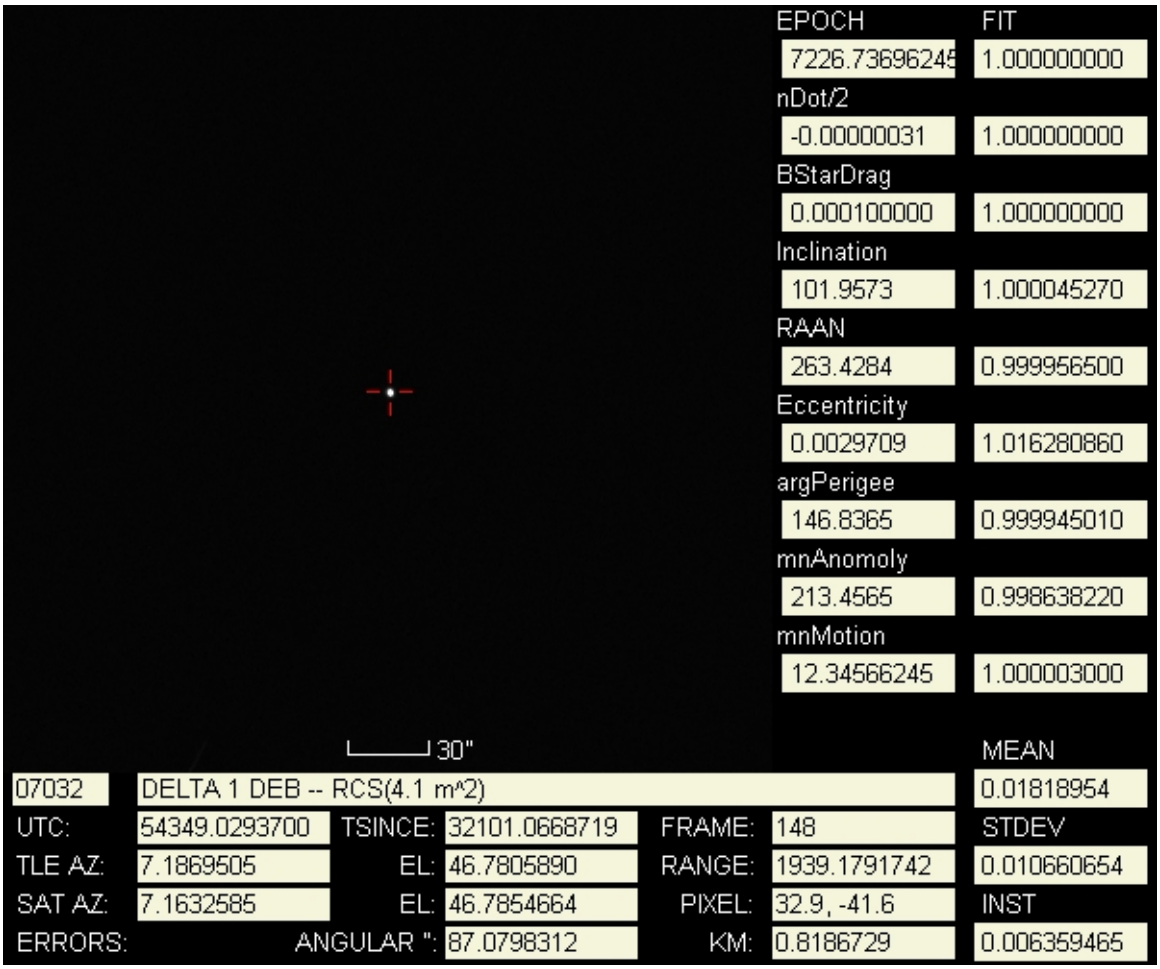

Figure 7 – Sample satellite track frame with measured satellite position and solved Keplerian elements.

Results

Figure 8 summarizes the tracking position errors of 07032 taken on September 5, 2007. Tracking commenced at elevation 35 degrees, culminated at 69 degrees elevation and terminated at 29 degrees elevation. Measure position error ranged from 0.69 km to 0.84 km. Using non-linear LSF the orbital position errors were reduced to less than 20 meters. For our purposes, position errors are calculated as the angular error vector in topocentric azimuth and elevation line of site look angles converted to a distance error using the SGP4 predicted range by the tangent of the angular position error. No attempt has been performed to analyze the position errors of the earth centered inertia (ECI) vectors and no conclusions can be drawn as to the magnitude of the specific along-track, cross-track, or radial obit errors. It is interesting to note, however, that our gross results are consistent with those predicted by Wiese and Sabol[7]

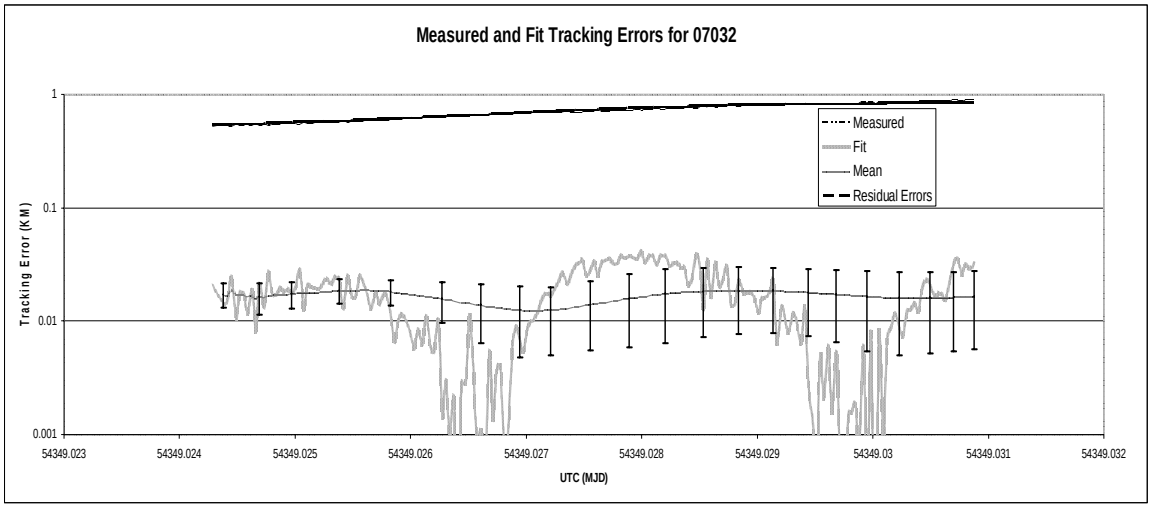

Figure 8 – Measured and fit position errors for 07032, September 5, 2007

Conclusions

The data presented is unverified and calibration satellites have yet to be tracked. However, the results are promising and we believe achieve the goal of this feasibility study. Based on the results achieved, we feel continued research and development is warranted. The authors recognize certain limitations of the current test site and equipment and recommend follow-up studies to include:

- Dark, transparent observatory site with horizon to horizon unobstructed visibility.
- Larger aperture acquisition telescope with high quality, low noise CCD camera.
- Verification of accuracy through observations of calibration satellites.
- Multi-pass, multi-site verification of orbital determination.
- Use of sophisticated orbital reduction techniques such as extended Kalman filters.
- Single site, single pass triangulated observations.
- Evaluation of different gimbal drive configurations, including low compliance direct coupled drives.

---

[1] Sabol, C., Kelecy, T., and Murai, M.. "Geosynchronous Orbit Determination Using the High Accuracy Network Determination System (HANDS)," AAS/AIAA Spaceflight Mechanics Conference, Wailea, Maui, HI, Feb. 8-12, 2004, AAS 04-216.

[2] Wallace, Patrick T. 2005. "SLALIB – Positional Astronomy Library 2.5-3" Starlink Project

[3] Wallace, Patrick T. 2006. "TPOINT Telescope Pointing Analysis System Version 10.8", TPoint Software.

[4] Henry, Michael F. 2006. "NORAD SGP4/SDP4 Implementations" http://www.zeptomoby.com/satellites/index.htm

[5] Hoots, Felix R., and R. L. Roehrich. 1980. "Spacetrack Report #3: Models for Propagation of the NORAD Element Sets." U.S. Air Force Aerospace Defense Command, Colorado Springs, CO.

[6] Kelso, TS. 2006. "Space Track TLE Retriever". http://celestrak.com/SpaceTrack/TLERetrieverHelp.asp

[7] Wiese, David, and Sabol, Chris. 2005. "Low Earth Orbit Prediction Accuracy Assessment Using Optical Data.". Advances in the Astronautical Sciences. Vol. 120, Part 1, pp. 589-607